Enhancing the performance of a building integrated compound parabolic photovoltaic concentrator using a hybrid photovoltaic cell

Damasen Ikwaba Paul*

Department of Electrical Engineering,
College of Engineering,
Chosun University,
309, Pilmun-daero, Dong-gu,
Gwangju 501-759, South Korea
Email: paul.ikwaba2018@gmail.com
Email: damasen.paul@out.ac.tz
*Corresponding author

Mervyn Smyth

Built Environment Research Institute,
Belfast School of Architecture and the Built Environment,
Ulster University,
Jordanstown Campus, Shore Road, Newtownabbey,
Co. Antrim, BT37 0QB, UK
Email: m.smyth1@ulster.ac.uk

Abstract: In this study, a hybrid photovoltaic (PV) cell consisting of high efficiency and low efficiency cells was designed and fabricated. For comparison, low efficiency single cell was also fabricated and both PV cells were evaluated within a compound parabolic concentrator (CPC). The fabrication of a hybrid cell was based on the simulation analysis which identified the regions with high energy concentration and low energy concentration in the CPC. Results indicates that the overall experimental daily power output of a hybrid PV cell on a clear sunny day and partial cloud day is higher than that of low efficiency single PV cell by 12% in both cases. On the other hand, the overall theoretical daily power output of a hybrid PV cell on a clear sunny day, partial cloud day and overcast day is also higher than that of low efficiency single PV cell by 11%, 10% and 13%, respectively.

Keywords: building integrated concentrating photovoltaic; compound parabolic concentrator; hybrid PV cell; low efficiency single PV cell; non-uniform illumination; experimental daily power output; theoretical daily power output; low-concentrating system; maximum power output.

Reference to this paper should be made as follows: Paul, D.I. and Smyth, M. (2020) 'Enhancing the performance of a building integrated compound parabolic photovoltaic concentrator using a hybrid photovoltaic cell', *Int. J. Renewable Energy Technology*, Vol. 11, No. 1, pp.49–69.

Biographical notes: Damasen Ikwaba Paul obtained his PhD in Photovoltaics Technology from Ulster University, UK in 2011. He holds a Master in Physics (Photovoltaics Technology) from the University of Dar es Salaam, Tanzania. In

his first degree (BSc with Education), he specialised in physics and mathematics. He is a permanent employee of the Open University of Tanzania but currently on sabbatical leave at the Department of Electrical Engineering, Collage of Engineering, Chosun University, South Korea. His research interests include photovoltaics technology, design, fabrication and testing of solar concentrators, optical analysis of photovoltaic concentrating systems and solar electricity application in remote areas. He has authored and co-authored over 27 publications in international and national peer reviewed journals.

Mervyn Smyth obtained a first Class BEng (Hons) in Building Services Engineering and PhD for solar energy research both from Ulster University, UK. He has over seven years of experience in the HVAC industry prior to taking up the position of Lecturer in Building Services Engineering at Ulster University. He has a particular interest in solar thermal and photovoltaic systems and has been involved in the design, development, fabrication and evaluation of various types of solar water heating units and photovoltaics. He has over 20 years of experience in the experimental characterisation of solar energy technologies under real and simulated conditions and has over ten years in the integration of passive solar systems and agri-frost protection, conducting numerous field experiments. He has authored over 65 publications to date, including his recently published book investigating the design principles of energy usage and solar augmentation in winery operation.

1 Introduction

Building integrated concentrating photovoltaic (BICPV) is a technique whereby a concentrator with a photovoltaic (PV) module is integrated in the building envelope mainly for electrical power generation. In the building envelope, concentrating systems can be integrated in different ways including flat roof mounting (Tripanagnostopoulos and Tripanagnostopoulos, 2008; Chemisana, 2011), sloping roof mounting (Tripanagnostopoulos et al., 2009; Chemisana, 2011), façade integration (Gajbert et al., 2007; Chemisana, 2011) and rear building side integration (Tripanagnostopoulos et al., 2009; Chemisana, 2011). However, the integrability of a concentrator in the building envelope depends on its geometric concentration ratio (C_g), the size of the system and the building architecture (Chemisana, 2011). In addition, it should satisfy the aesthetic criterion formulated by the International Energy Agency Photovoltaic Power System Task VII (Reijenga, 2000; Chemisana, 2011). These aesthetic criterion are architecturally pleasing design, well-engineered and innovative design, good composition of colours and materials as well as conformity to the context of the building.

Contrary to conventional photovoltaic systems or flat panel building integrated systems, concentrating photovoltaic systems use lenses or reflectors to focus sunlight onto a small area solar cells. By increasing the light flux on the PV module, significant improvement in electrical power output is achieved due to the fact that the current increases proportional to the concentrated intensity (Paul et al., 2013). In addition, the optical element in a concentrating system is cheaper than solar cells which are expensive, thus leading to potential saving (Luque et al., 2006). Other advantages of BICPV systems over conventional flat panel building integrated systems include better use of space and option of recycling the component materials and use of less toxic products associated with production of PV cells (Chemisana, 2011; Baig et al., 2015).

Solar concentrators are generally categorised as refractive or reflective. The former can be achieved by lenses whilst the later uses reflectors. Both refractive and reflective concentrators may be further classified as high concentrating systems (C_g > 100x), medium concentrating systems (10x < C_g < 100x) or low concentrating systems (C_g < 10x) (Swanson, 2003; Chemisana, 2011; Micheli et al., 2013). Although high concentrating systems result in higher light intensities on the PV cells and hence lower cost per kWh produced, but they require a system to track the sun, whereas low concentrating systems can be static (Cardona, 2001; Chemisana, 2011). In addition, low concentrating collectors are less expensive than high concentrators as they do not require solar tracking devices. Furthermore, manufacturing costs are cheaper because their components are simpler and require low-cost in maintenance (Cardona, 2001). These characteristics of low concentrating systems facilitate their placement at any location in the building.

Over the past two decades, several designs of low concentrating photovoltaic systems for building integration have been experimentally tested. Findings indicate that it is possible to increase power output by using BICPV systems. The concentrators which have been extensively investigated include linear asymmetric compound parabolic concentrator, CPC (Zacharopoulos et al., 2000; Mallick et al., 2004, 2006; Mallick and Eames, 2007; Sharma et al., 2016), highly asymmetric CPC with only one upper reflector (Gajbert et al., 2007), asymmetric lens-walled symmetric CPC (Guiqiang et al., 2013; Xuan et al., 2017), 3D crossed compound parabolic concentrator (Mammo et al., 2012), Symmetric Elliptical Hyperboloid concentrator (Baig et al., 2015), 3D Square Elliptical Hyperboloid concentrator (Sellami et al., 2012), Window Integrated Concentrating Photovoltaic (Sellami and Mallick, 2013), mirror symmetrical dielectric totally internally reflecting concentrator (Muhammad-Sukki et al., 2014) and planar reflectors such as V-trough (Maiti et al., 2012). However, most of these concentrators do not produce uniform flux on the PV module (Paul et al., 2013). For a standard PV module in which cells are connected in series, non-uniform flux distribution causes a reduction in power output and electrical conversion efficiency due to the fact the current of the entire PV module depends on the least-illuminated PV cell(s) (Greenman, 1980; Rauschenbach, 1980; Pfeiffer and Bihler, 1982). In addition, non-uniform illumination causes heating of a PV cell along the surface as well as non-uniform temperature profiles across the PV module, causing further reduction in power output and electrical conversion efficiency (Nasby and Sanderson, 1982; Paul et al., 2019).

Several techniques have been investigated so as to enhance the electrical performance of a PV module in which the energy flux on the surface is non-uniformly distributed. These include distortions in reflecting surfaces of the concentrator (Greenman, 1980), bypass diode (Edenburn and Burns, 1981; Suryanto-Hasyim et al., 1986; De Boer et al., 2003), special design of concentrator profiles (Greenman, 1980; Kurzweg, 1980; Gupta et al., 1981; Jorgensen and Wendelin, 1992; Singh and Liburdy, 1993), diffuse reflector materials (Hall et al., 2005; Nilsson et al., 2007; Hatwaambo et al., 2008), special concentrator cells design (Baig et al., 2012), secondary concentrator optical element (Baig et al., 2012) and special PV module design (Paul et al., 2013).

In the study carried out by Paul et al. (2013), a novel isolated cells PV module was designed, fabricated and experimentally characterised with and without the CPC. It was found that the fabrication of a PV module with isolated cells and the effect of non-uniform illumination resulted in higher power output for cells located in peak energy concentration regions and lower power output for cells in the lower illumination region of the CPC. In such a case, it is economically viable to design and fabricate a PV cell or module in which high efficiency (HE) PV cells are placed in the highly illuminated regions and low efficiency (LE) cells in the lowest illuminated regions of the CPC. Conversion efficiency is an important parameter in solar cells because the higher the efficiency, the less surface area it takes for the PV modules to meet the energy requirements. At the moment, the most efficient PV cells in production are crystalline Silicon solar cells that achieve typical efficiencies of 26.6% and a module conversion efficiency of 24.4% (Liu et al., 2018; Yamamoto et al., 2018). These cells are fabricated by combining rare semiconductor materials with differing band gaps such as germanium, gallium and indium to convert a broader range of the solar spectrum into energy. The most top layer of the solar cell has the largest band gap so that only the most energetic photons are absorbed in this layer. Less energetic photons must pass through the top layer since they are not energetic enough to generate electron-hole pairs in the material. These photons are absorbed by the lower solar cell layers which mean that less energy is lost.

Fabrication of hybrid PV module consisting of HE and LE solar cells ensures maximum power output from the overall PV module but at low cost due to the fact that the area occupied by high quality cells (which are more expensive) is less than the area occupied by LE cells (which are cheaper). However, for a stationary building integrated concentrator, the challenge in fabricating such a PV module lies in identifying the positions where high energy flux is concentrated over the whole year so that HE cells can be installed in these areas.

Therefore, this study had two main objectives:

1 to design and fabricate a novel PV cell consisting of HE and LE cells, hereafter called ‘hybrid PV cell

2 to analyse the electrical power output of a hybrid PV cell and compare the results with that of a LE single PV (LESPV) cell.

Both PV cells were evaluated in a low concentrating stationary symmetric CPC suitable for integration into various parts of a building envelope.

2 Materials and methods

2.1 Design and fabrication of compound parabolic photovoltaic concentrator

In this study, a symmetric 2-dimensional (2D) CPC was designed (Figure 1) and fabricated (Figure 2). The CPC with an acceptance half-angle (θ_a) of 30° which corresponds to concentration ratio of 2.0 that can be easily integrated into the existing building structure was chosen. After truncation, the entrance area reduced to 303 mm (Figure 1) while the exit aperture remained the same (156 mm), thus making geometric concentration ratio of 1.96. The CPC was truncated to reduce fabrication cost due to the fact that as the height of the CPC increases, more reflector materials are required and hence higher fabrication cost (Rabl, 1976). In addition, large reflector height in the CPC results in higher reflections losses (Rabl, 1976). To eliminate the end-loss effect (Whitfield et al., 1999), the length of the CPC was made longer (800 mm long) than the length of the two PV cells joined together. Aluminium sheet with reflectivity of 0.91 was used as reflector material.

Figure 1 Detail design dimensions of a symmetric 2D CPC and fabrication materials

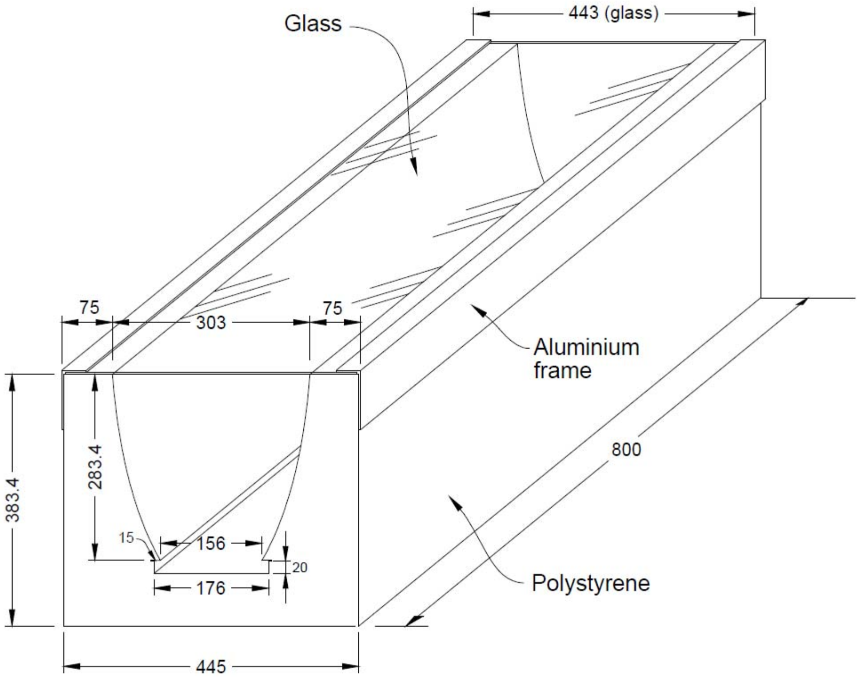

Note: All dimensions are in mm.

Figure 2 Fabricated symmetric 2D CPC with an opti-white glass as aperture cover (see online version for colours)

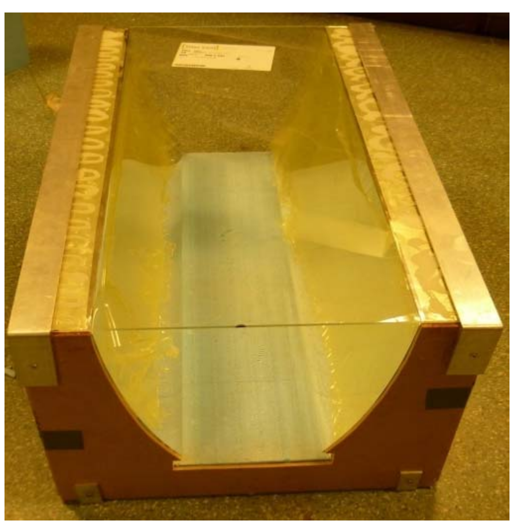

2.2 Design and fabrication of a hybrid photovoltaic cell

In order to design a hybrid PV cell to be placed underneath of a symmetric 2D CPC shown in Figure 2, simulation analysis using ray trace program (Zacharopoulos, 2001) was carried out to identify the areas with high annual solar radiation concentration in the CPC receiver as well as the width of each HE PV cell strip. It was found that to design such a hybrid PV cell, the receiver with dimensions of 156 mm × 156 mm (that fits exactly in the exit aperture of the CPC in Figure 2) has to be divided into 10 sections (as indicated in Figure 3), each section has different width but the same length. Of the 10 sections, three sections had much less area than others and were designed to be occupied by the connecting tabs. Figure 3 shows the positions and dimensions of HE PV cell stripes, LE cells and connecting tabs. From these dimensions, the area occupied by HE PV cell stripes and connecting tabs is 33% and 5% (of the total hybrid PV cell area), respectively.

Figure 3 Design of a hybrid PV cell showing the location of HE and LE PV cells* (see online version for colours)

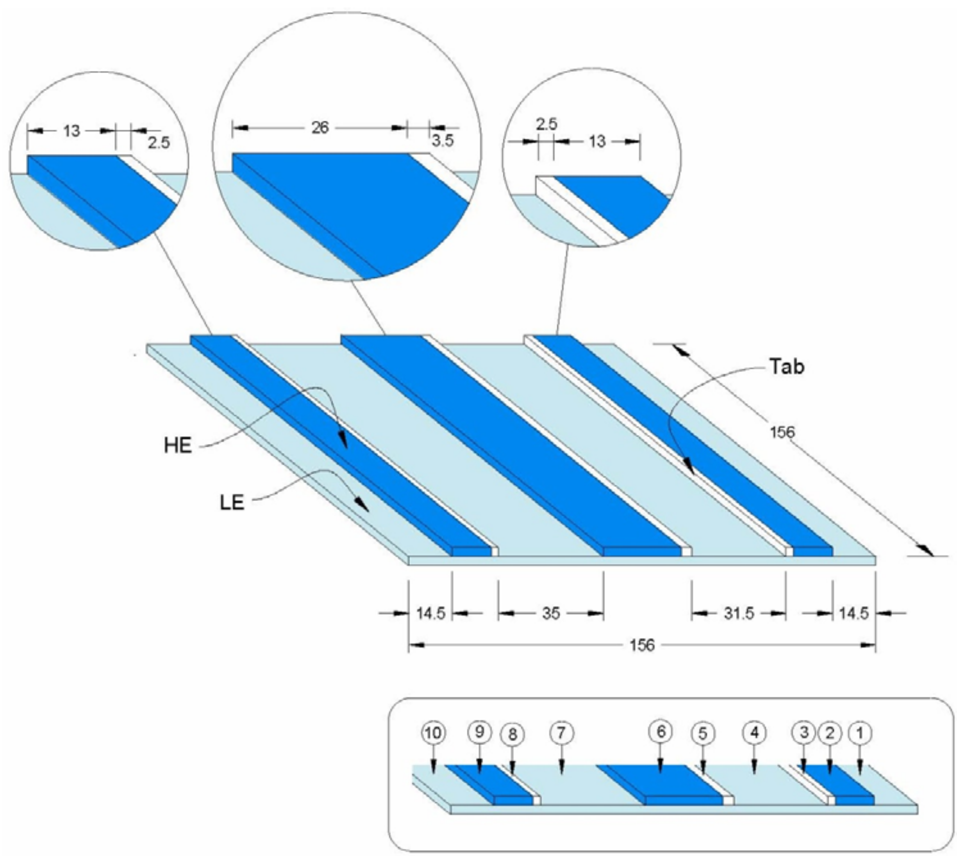

Notes: All dimensions are in mm.
The hybrid PV cell consists of 10 different sections (numbered from 1 to 10).

After identifying the areas to be occupied by LE and HE PV cells as well as connecting tabs in the hybrid cell, the next task was to fabricate a hybrid PV cell. In fabricating this PV cell, LE PV cell was mono-crystalline cell from Blue-Sky Technology (China) (Anon, 2010a) whilst HE PV cell was Bosch M 2BB mono-crystalline cell from Germany (Anon, 2010b). Since the stripes of HE PV cells have to be installed in the areas of the receiver with high annual energy concentration, as identified in Figure 3, a single HE PV cell was cut (using a FB1500 Laser Cutting Machine) into stripes of different widths depending on the width of the area occupied by the high annual solar energy.

Figure 4 Fabricated hybrid, (a) PV cell (b) LESPV cell (see online version for colours)

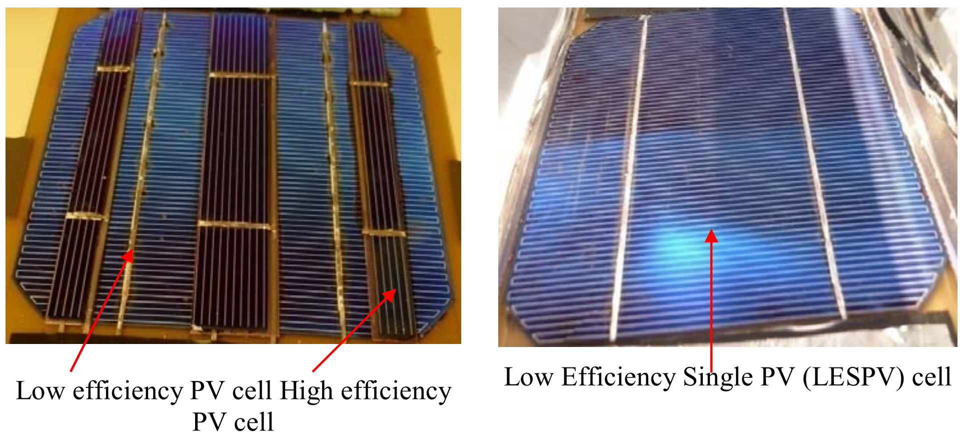

(a) (b)

For direct comparison with a hybrid PV cell, LE single PV (LESPV) cell was also fabricated. Figure 4 shows the photographs of the two fabricated PV cells.

For better heat dissipation from the PV cells, a single-sided Insulated Metal Substrate (IMS) board, was used as a support base in the fabrication of both LESPV and hybrid PV cells. To dissipate the heat away from the PV cell to the IMS board and then outside the PV cell, the interface between the IMS board and the PV cell requires the use of a good thermal heat transfer adhesive. This is due to the fact that any air gaps or other materials that exist between a PV cell and the IMS board acts as an insulator thus preventing heat from the PV cell and hence a reduction in electrical performance (Mallick et al., 2007). In this PV cells fabrications, ACC Silicone thermally conductive adhesive sealant was used to attach the PV cell to the IMS board. To form a hybrid PV cell, both HE and LE cells were electrically connected using connecting leads. To avoid short-circuiting between the LE PV cell and HE PV cell stripes, which could cause ohmic loss and overheating, a doubled-sided (0.4 mm thick) IMS board was sandwiched between the two PV cells. In addition, the double-sided IMS board ensured that the photons with energy less than the band gap energy of the HE PV cell do not reach the LE PV cell.

Table 1 Cost breakdown for fabricating LESPV cell and hybrid PV cell

Type of material	*Quantity and unit*	*Price per unit ($)*	*Total cost ($)*	*Total cost ($)*
			LESPV cell	*Hybrid cell*
LE mono-crystalline solar cell (156 mm × 156 mm)	1 piece	3.02	3.02	0
LE mono-crystalline solar cell (156 mm × 104 mm)	3 pieces of stripes	2.01	0	1.89
HE Bosch mono-crystalline solar cell	3 pieces of stripes	0.72	0	0.72
Single-sided insulated metal substrate (IMS) boards (166 mm × 166 mm)	2 pieces	1.50	1.50	1.50
Double-sided IMS board (0.4 mm)	1 piece	0.30	0	0.30
ACC silicone sealant	1 tube	8.50	4.25	4.25
Silver solder	1 piece	4.10	2.05	2.05
Tab ribbon 2 mm wide	1 piece	5.00	2.50	2.50
Flux pen	1 piece	1.20	0.60	0.60
Solar cable (100m reel)	1 piece	10.75	5.38	5.38
Junction box	2 pieces	1.50	1.50	1.50
Labour	Man-day	0.01 $/min	0.01	0.02
Total			20.81	20.71

Table 1 shows the total cost of fabricating one unit of each type of the PV cell. The cost is almost the same ($20.81 for LESPV cell and $20.71 for hybrid cell) but this is an overestimated cost because in reality, materials such as silicone sealant, silver solder and flux pen will remain after fabricating one unit solar cell. The remaining materials will be used in the fabrication of other units and this will results into cost reduction.

2.3 Outdoor experimental test procedure

A series of outdoor experimental tests were conducted to analyse the electrical power output of a hybrid PV cell and compare the results with that of a LE single PV (LESPV) cell both placed underneath of a low-concentrating symmetric 2D CPC as shown in Figure 5. The electrical power outputs of the two PV cells were analysed for three different solar conditions: clear sky, partial cloudy and overcast days. These days were deliberately selected so that the results could represent the variations in solar irradiance typical in any given year. The experimental tests were set at the Centre for Sustainable Technology laboratory, Ulster University, Jodardstown Campus (54.6° N, 5.9° W), Belfast. Since the highest solar insolation and clear sky conditions in this area occurs during summer time (Anon, 2006), the experimental tests were carried out during June to July. For direct comparison of the results, the PV cells were tested simultaneously in a single CPC oriented North-South and tilted at 54° as shown in Figure 5.

Figure 5 Outdoor experimental set-up (see online version for colours)

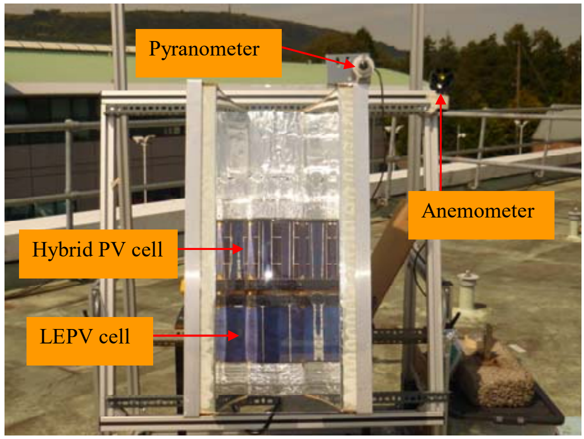

In this experiment, total solar radiation was measured by a pyranometer fixed on the aperture of the CPC as shown in Figure 5 whilst diffuse irradiance was measured by shading another pyranometer from the direct normal irradiance. The ambient and cell temperatures were measured by using 561 Fluke Infrared and contact Thermometer while wind speed was measured by a digital anemometer (fixed on the aperture of the CPC as shown in Figure 5). For each PV cell, the operating cell temperature was taken at three different points (across the middle of the PV cell) and plotted as the average of the three temperature readings. During experimental test and analysis, the PV cells were identified as LE PV (LESPV) cell and hybrid PV cell. For each PV cell, current and voltage were measured manually using a fixed resistive load method (Osterwald et al., 2006; Paul, 2011).

2.4 Procedure for determination of theoretical daily power output

In this research, theoretical power outputs from both PV cells (a hybrid PV cell and LESPV cell) were also analysed and results were compared. To determine the theoretical daily power output from a hybrid PV cell and LESPV cell, a simulation program developed by Zacharopoulos (2001) was used. This program uses typical location beam and diffuse hourly solar radiation data to predict, among others, hourly, daily and annual variations of solar energy collected by any BICPV. Therefore, beam and diffuse solar irradiance used in this simulation were measured during experimental tests described in section 2.3. The other inputs to the simulation program included the position of the sun in the sky (latitude and longitude), concentrator acceptance angle, orientation of the concentrator (N-S), concentrator tilt and azimuth angles as well as transverse incidence angles of direct and diffuse irradiance sunrays.

Since the hybrid PV cell consisted of 10 sections of different sizes and electrical conversion efficiencies, the theoretical daily power output, $P_{Daily}(\text{Hybrid})$, was calculated based on the hourly incident energy on each section, $(E_{H\text{-}i})$, the size of the section and the electrical conversion efficiency of each section, as follows:

$$P_{Daily}(\text{Hybrid}) = \sum P_{Hour}(\text{Hybrid}) \quad (1)$$

where

$$P_{Hour}(Hybrid) = \sum_{i=1}^{i=10} P_{Hour}(i) \tag{2}$$

and

$$P_{Hour}(i) = G_B \times C_B \times A_i \times \eta_i + G_D \times C_D \times A_i \times \eta_i \tag{3}$$

where G_B, G_D, C_B and C_D are the beam solar irradiance on the aperture of the CPC, diffuse solar irradiance on the aperture of the CPC, beam energy concentration on the i^{th} section of the hybrid PV cell and diffuse energy concentration on the i^{th} section of the hybrid PV cell, respectively. $P_{Hour}(i)$ is the hourly electrical power produced by the i^{th} section of the hybrid cell, $P_{Hour}(Hybrid)$ is the total electrical power of the hybrid PV cell at every hour, A_i is the area of the i^{th} section of the hybrid PV cell and η_i is the conversion efficiency of the i^{th} section of the hybrid PV cell.

For sections of the hybrid PV cell occupied by connecting tabs (as illustrated in Figure 3), $\eta_i = 0$ thus, $P_{Hour}(i) = 0$.

For the LESPV cell, the theoretical daily power output, $P_{Daily}(LESPV)$, was calculated as:

$$P_{Daily}(LESPV) = \sum P_{Hour}(LESPV) \tag{4}$$

where

$$P_{Hour}(LESPV) = G_B \times \eta_{optical\text{-}B} \times C_g \times \eta_{LESPV} + G_D \times \eta_{optical\text{-}D} \times C_g \times \eta_{LESPV} \tag{5}$$

where $\eta_{optical\text{-}B}$ and $\eta_{optical\text{-}D}$ are the optical efficiency for beam solar irradiance and optical efficiency for diffuse solar irradiance, respectively and C_g is the geometrical concentration ratio of the CPC.

In calculating the theoretical daily power output of both PV cells, diffuse solar irradiance was assumed to be isotropically distributed (Prapas et al., 1987).

3 Results and discussions

3.1 Experimental daily power output of the PV cells

3.1.1 Power output of the PV cells on a clear sunny day

Figure 6 shows the variations of total and diffuse solar irradiance on the aperture of a CPC as well as the variations of power output between LESPV cell and a hybrid PV cell on a clear sunny day. Throughout the experimental test period, the total solar irradiance was high, indicating a clear sky day. It can be observed from Figure 6 that the maximum solar irradiance was about 942 W/m^2 (at 13:40 hour) and, due to high degree of the atmospheric transparency, the diffuse solar irradiance remained below 200 W/m^2 for most of the experimental duration. This high solar irradiance caused high operating cell temperatures for both PV cells as shown in Figure 7. However, as it can be seen from Figure 7, there is no significant differences in operating cell temperature between LESPV cell and a hybrid PV cell. As a result, the effect of operating cell temperature on the power output was the same for both PV cells.

Figure 6 Comparison of electrical power output between LESPV cell and a hybrid PV cell on a clear sunny day (see online version for colours)

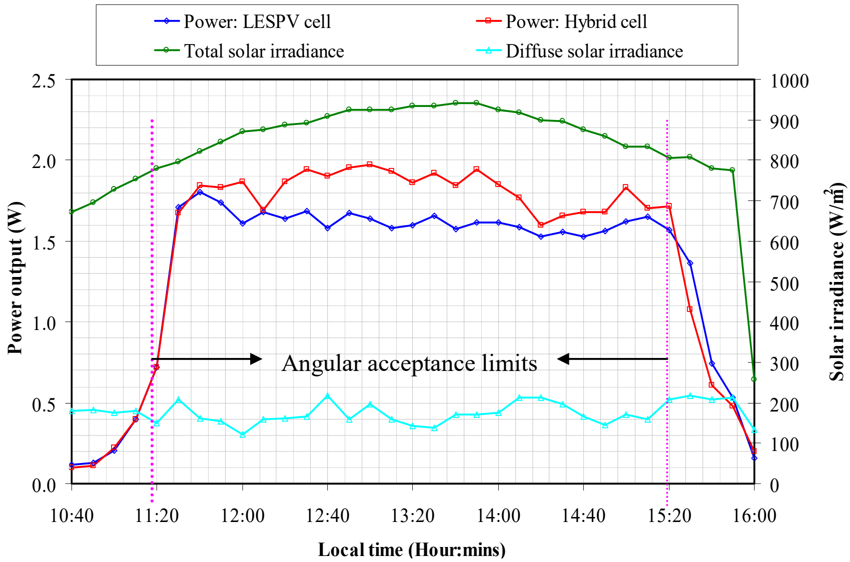

Note: The measured solar irradiance has also been included for direct comparison.

Figure 7 Variation in operating cell temperatures (for LESPV cell and a hybrid PV cell) and ambient temperature during the experimental test on a clear sunny day (see online version for colours)

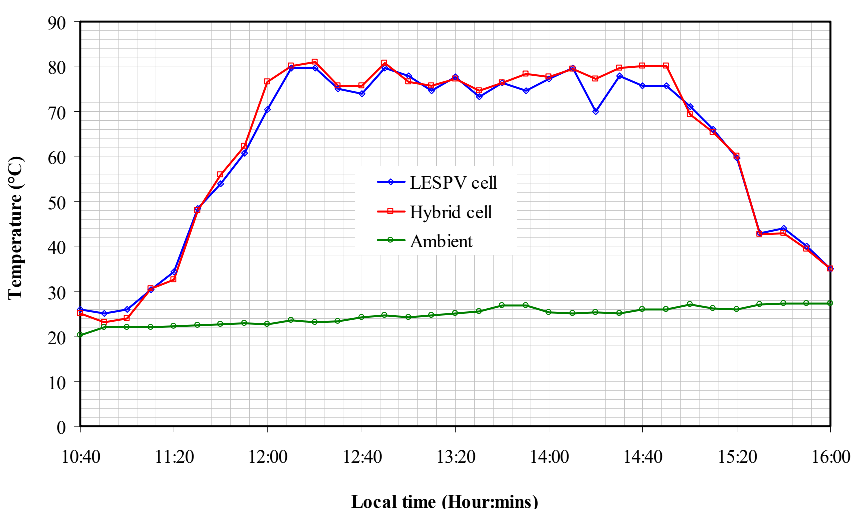

From Figure 6, it can be seen that for the solar irradiance incident outside the acceptance limits of the CPC (i.e., before 11:20 and after 15:20 hours), there is no significant difference in power output between the two PV cells. However, when the incidence angle of the incident solar irradiance was within the acceptance limits of the CPC (i.e., between 11:20 and 15:20 hours), the power produced by a hybrid PV cell was higher than that of a LESPV cell. During this time, the difference in instantaneous power output between the two PV cells varied from about 2% at 11:40 to 22% at 13:10 (near solar noon, which was 13:20). The difference in power was not constant due to variations of energy flux distribution on the cells as the incidence angle changes with the sun's movement across the sky. When the comparison is made based on the total power output produced while the angle of incidence was within the acceptance of the CPC (i.e., between 11:20 to 15:20 hours), it was found that the power output of a hybrid PV cell is about 12% higher than that of LESPV cell.

3.1.2 Power output of the PV cells on a partial cloudy day

The influence of clouds is an important parameter that affects the performance of a building integrated concentrating photovoltaic system. This is due to the fact that the presence of clouds in the sky decreases the amount of global solar irradiance and increases the amount of the diffuse irradiance. Thus, in addition to a significant drop in power output of the PV module, the diffuse solar irradiance modifies the distribution profiles of the incident energy on the surface of the PV module. To examine the effect of clouds on the performance of a hybrid PV cell, an experimental test was carried out during one of the partial cloudy days. Figure 8 shows the variations of total and diffuse solar irradiance as well as the variations of power output for the two PV cells. It can be seen that, due to clouds effect, the solar irradiance before and after solar noon is not symmetrical and the value of the diffuse irradiance was always higher than 200 W/m^2 most of the time of the experimental test.

Figure 8 Comparison of electrical power output between LE single cell and a hybrid PV cell on a partial cloudy day (see online version for colours)

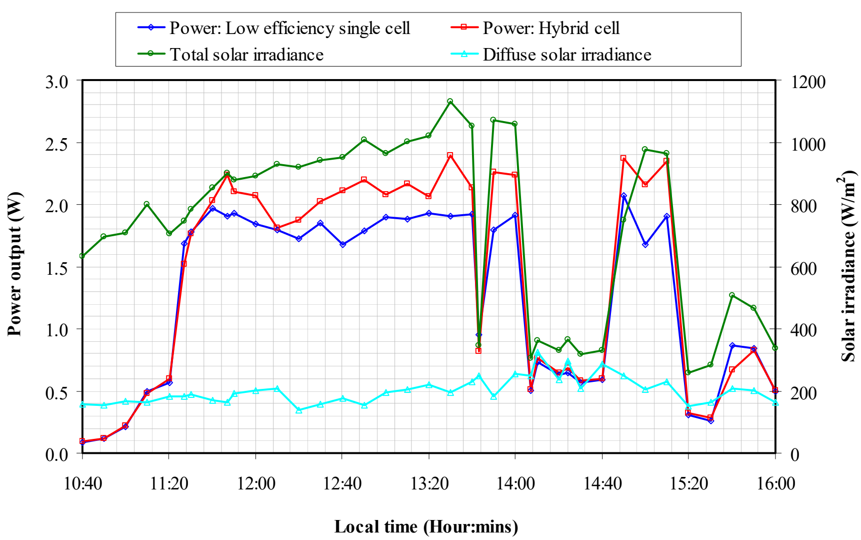

Note: The measured solar irradiance has also been included for direct comparison.

Figure 8 also shows a comparison of power output between LE single cell and a hybrid PV cell. It can be seen that when the incidence angle of the solar irradiance is higher than the acceptance half-angle of the CPC (i.e., between 10:40 (+40°) to 11:10 (+32.5°) and between 15:30 (–32.5°) to 16:00 (–40°)), there is no significant difference in power output between the PV cells. The reason in that, at these times, most of the accepted solar irradiance is mainly diffuse irradiance and uniformly distributed over the surface of each PV cell. As shown in Figure 8, during cloudy hours, for example between 14:10 to 14:40 hours, both PV cells produced equal amount of electrical power, indicating that there is no benefit in using a hybrid PV cell during this period. However, when the sun shines again, due to high concentration energy on the HE cells, the hybrid PV cell performs better than LE single PV cell. For example, at 13:30 and 13:50 hours, the power output produced by a hybrid PV cell was higher than that of LE single PV cell by about 27%. On the other hand, when the comparison of the PV cells is made based on the total hours of the experimental test (5.3 hours), it was found that LE single PV cell produced 47.7 W while a hybrid PV cell produced 52.7 W. This means an energy improvement of about 10% when using a hybrid PV cell. This improvement increases to about 12% when the comparison is based on the standard collection period of a CPC with acceptance half-angle of 30° in the N-S orientation (which is four hours).

Figure 9 Variations of operating cell temperatures for LE single PV cell and a hybrid PV cell as well as ambient temperature during the experimental test on a partial cloudy day (see online version for colours)

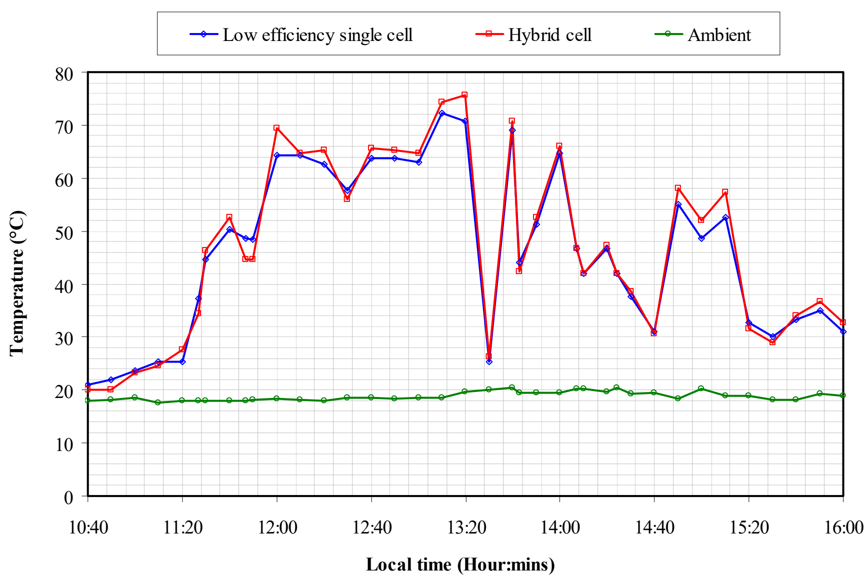

Figure 9 shows the variations of operating cell temperatures and ambient temperature over the experimental test period during a partial cloudy day. It can be seen that both PV cells had almost the same operating temperatures, which means that the observed differences in power output between the PV cells (Figure 8) was not due to their differences in operating cell temperature.

3.1.3 Power output of the PV cells on overcast weather condition

Overcast weather is the meteorological condition of clouds obscuring all the sky for a specific time, which may range from few hours to the whole day. It differs from both clear sky and partial cloudy days in the sense that during overcast time, most of the incident solar irradiance is diffuse. To find out if a hybrid PV cell performs better than a LE single PV cell on overcast weather conditions; an outdoor experimental test was carried out in one of the overcast days. Figures 10 and 11, respectively, show the variations of total, beam and diffuse solar irradiance and the comparisons of power output between LE single PV cell and a hybrid PV cell during the experimental test on overcast day. With regards to solar irradiance variations (Figure 10), it can be seen that before 12:20, the weather condition was characterised by sunny-cloudy as illustrated by low and high total solar irradiance. For example, at 11:25 the total solar irradiance was about 300 W/m^2 while at 11:55 it was over 1,000 W/m^2. However, between 12:15 and 16:00 hours, the sky was completely full of clouds as demonstrate by both low total solar irradiance and higher diffuse irradiance than the beam irradiance. As a result, the maximum operating cell temperature of both PV cells during overcast hours, as illustrated in Figure 12, was less than 25 °C. It is also shown in Figure 12 that there is no significant difference in operating cell temperatures between LE PV single cell and a hybrid PV cell. Thus, the effect of temperature on the power output was the same for both PV cells.

Figure 10 Variations of total, beam and diffuse solar irradiance during the experimental test on overcast day (see online version for colours)

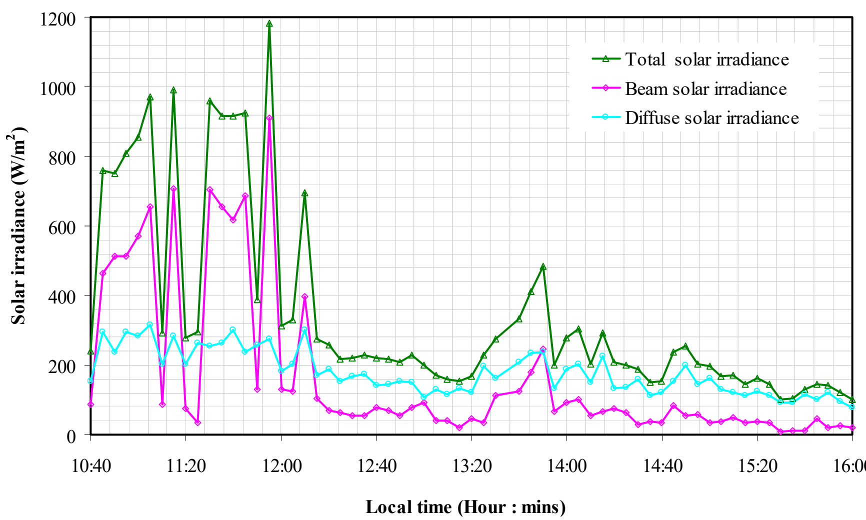

As shown in Figure 11, there is no significant difference in instantaneous power output between LE single PV cell and a hybrid PV cell during most time of the experimental test. The reason is that, most of the times, high energy was concentrated on LE cell sections in a hybrid PV cell.

Figure 11 Comparison of the power output between LE single PV cell and a hybrid PV cell during the experimental test on overcast day (see online version for colours)

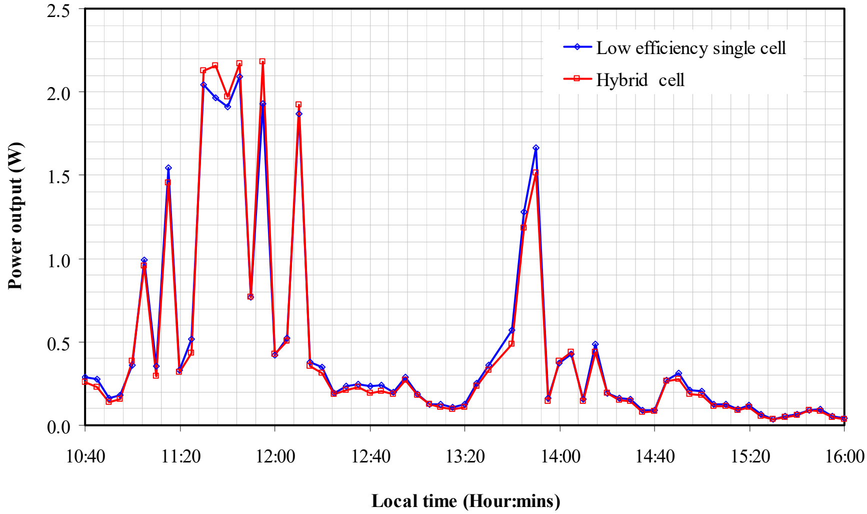

Figure 12 Variations of operating cell temperatures (LE single cell and hybrid cell) and ambient temperature during the experimental test on overcast day (see online version for colours)

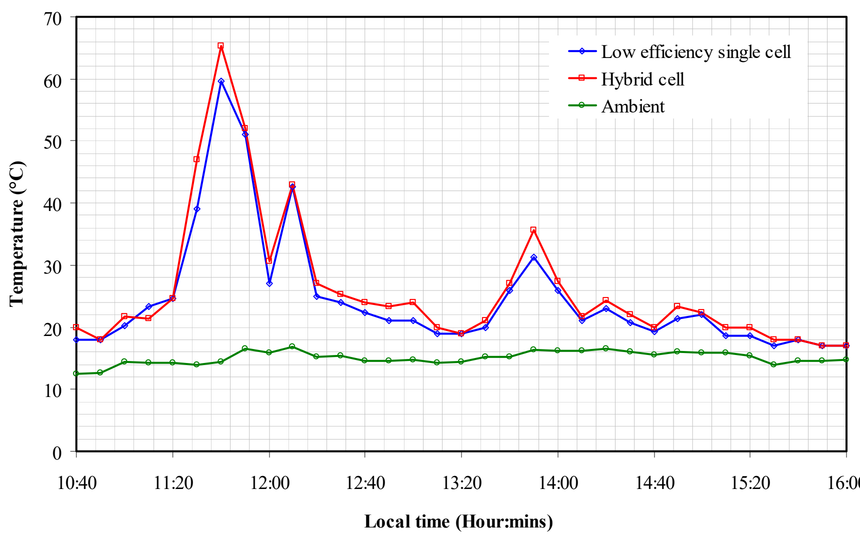

3.2 Theoretical daily power output of the PV cells

Figure 13 shows the comparison of theoretical daily power output of LE single PV cell and a hybrid PV cell for different weather conditions: clear sunny day [Figure 13(a)], partial cloudy day [Figure 13(b)] and overcast day [Figure 13(c)]. It is observed from the three figures that the theoretical daily power output for a hybrid PV cell is always higher than that of LE single PV cell, even when the incidence angle of the solar irradiance is higher than the acceptance half-angle of the CPC (i.e., between 10:40 to 11:10 hours when θ_{in} >+ 30° and between 15:10 to 16:00 hours when θ_{in} >– 30°. However, as it was observed in the case of the experimental results (Figure 6), significant difference is seen during a clear sunny day or hours with sunshine as shown in Figure 13(a) and Figure 13(b) between 11:40 and 14:00 hours. This is due to high current generated from the HE PV cell stripes when high energy is concentrated on these areas thus increasing the overall power output of the hybrid PV cell. Previous study has shown that for a PV module with cells individually connected, the current generated by each cell is proportional to the incident energy (Paul et al., 2013).

Figure 13 Comparison of theoretical daily power output between LE single PV cell and a hybrid PV cell on three different weather conditions (see online version for colours)

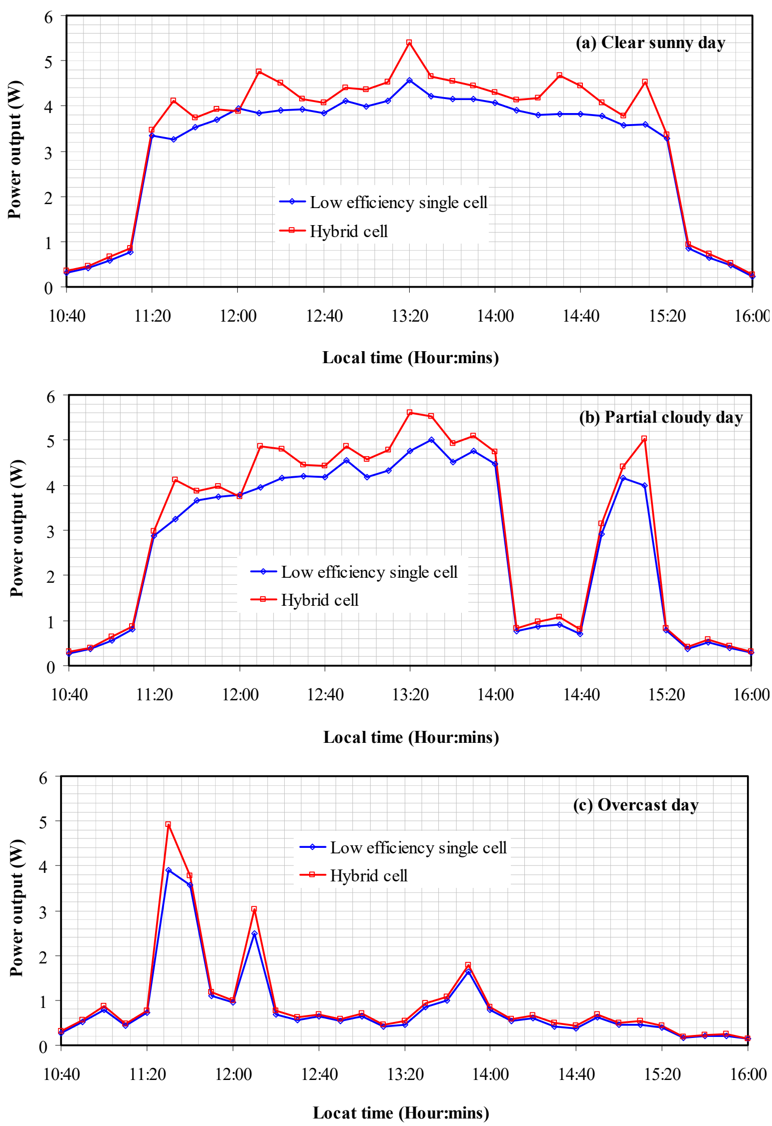

Figure 14 Variation of incident energy on each section of the hybrid PV cell during overcast day. HE and LE represents high and LE cells, respectively, whereas tabs are the areas occupied by tin/lead connecting taps (see online version for colours)

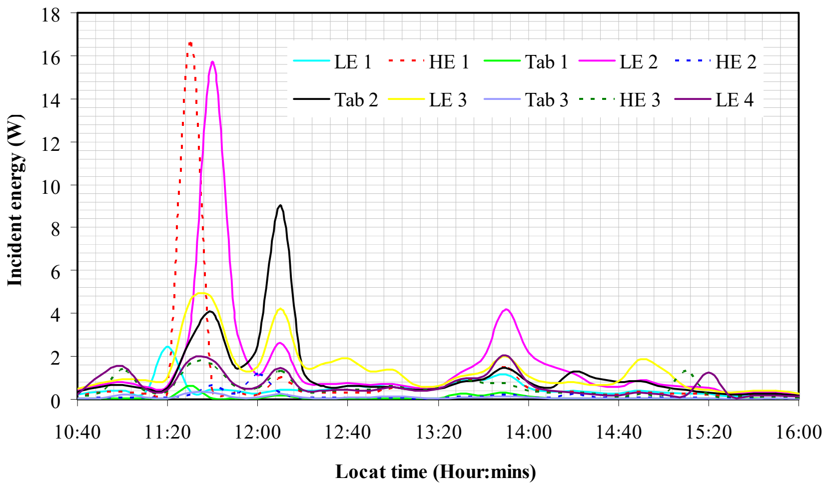

Figure 15 Comparison of theoretical daily power output between LE single PV cell and a hybrid PV cell on three different weather conditions (see online version for colours)

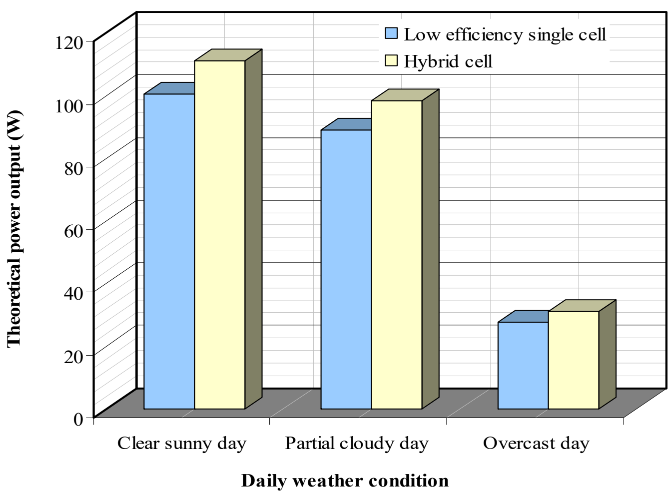

For partial cloudy and overcast days, Figure 13(b) (from 14:00 to 16:00 hours) and 13(c), respectively, the variation of power output between LE single PV cell and a hybrid PV cell is not significant, except for high solar irradiance [e.g. between 15:00 and 15:20 hours in Figure 13(b) and between 11:20 and 11:40 hours in Figure 13(c)]. The reason is that, most of the time, as illustrated in Figure 14, high energy was concentrated on LE cell sections for a hybrid PV cell. However, if the comparison is made based on the total time of the test rather than on hourly basis, the overall theoretical daily power output for the hybrid PV cell is much higher that of LE single PV cell. Figure 15 shows the comparison of the total power output between LE single PV cell and a hybrid PV cell for different weather conditions whilst Table 1 illustrates the differences (in percentage) between the two PV cells. The percentage difference in power output shown in Table 2 was calculated based on the total time of the test and the time when the incidence angle of the solar irradiance is within the acceptance half-angle (θ_a = 30°) of the CPC. As shown in Table 2, the overall theoretical daily power output of a hybrid PV cell on a clear sunny day, partial cloud day and overcast day is higher than that of LE single PV cell by about 11%, 10% and 13%, respectively. These values do not change even if the power output is calculated based on the standard collection time of the CPC with θ_a = 30° in the N–S orientation.

Table 2 Variation of theoretical daily power output between LE single PV cell and a hybrid PV cell as the function of weather conditions

Type of a PV cell	*Power output (W), calculated based on the total time of the test*			*Power output (W), calculated based on the standard collection time of the CPC with θ_a = 30°*		
	Clear sunny	*Partial cloudy*	*Overcast*	*Clear sunny*	*Partial cloudy*	*Overcast*
Lowe efficiency single PV cell	100.50	89.06	27.57	96.18	85.46	24.84
Hybrid PV cell	111.09	98.36	31.08	106.34	94.39	28.05
Difference (%)	10.54	10.45	12.73	10.56	10.45	12.91

4 Conclusions

A series of outdoor experimental tests were conducted to analyse the electrical power output of a hybrid PV cell and compare the results with that of a LE single PV cell both placed underneath of a low-concentrating symmetric 2D CPC. The experimental results indicate that, on a clear sunny day the power produced by a hybrid PV cell was always higher than that of LE single PV cell. The instantaneous power output varied from about 2% at 11:40 to 22% at 13:10 hours. However, when the comparison was made based on the total time of the experimental test; it was found that the power output for a hybrid PV cell was about 9% higher than that of LE single PV cell. This difference increased to about 12% when it was compared based on the total power produced when the incidence angle of the solar irradiance was within the acceptance half-angle of the CPC.

On a partial cloudy day, the total power produced by a hybrid PV cell was higher than that of LE single PV cell by about 10%. This improvement increased to about 12% when the comparison was made based on the standard collection period of a CPC with acceptance half-angle of 30° in the N-S orientation (which is four hours). This indicates that the hybrid PV cell also works in climates with very cloudy and diffuse solar irradiance conditions. The experimental result on overcast day indicated LE single PV cell performed better than a hybrid PV cell by about 9%. Therefore, the effect of energy concentration is less relevant during overcast days, limiting the use of a hybrid PV cells to sunny and partial cloudy days.

When the PV cells was evaluated based on the simulation results, it was found that the overall theoretical daily power output of a hybrid PV cell on a clear sunny day, partial cloud day and overcast day was higher than that of LE single PV cell by about 11%, 10% and 13%, respectively.

In general, both experimental and simulation results had shown that the total power produced by a hybrid PV cell was higher than that of LE single PV cell. The percentage of variations depends on the weather condition of a particular day. Therefore, the use of a hybrid PV cell and a symmetric 2D static low-concentrating CPC designed for building integration has a potential to significantly increase the annual electrical production compared to a standard PV module.

References

Anon (2006) *Sustainable Energy Systems, Report on Energy Efficient and Renewable Energy Systems Planning and Recommendations for their Successful Application*, Six Framework Programme, Policy, DR 1.1 TREN/05FP6EN/S07.43964/513481 [online] http://www.scribd.com/doc/6609997/Report-on-Energ-Efficient.

Anon (2010a) *High Performance – Stable Yields*', Bosch Solar Cell M 2BB, Bosch Solar Energy AG Wilhelm-Wolff-Straße 23 99099, Erfurt, Germany.

Anon (2010b) *Mono-Crystalline PV Cell Technical Data Sheet*, Bluesky Led Technology Co., Ltd., 1608 No.1 Building, Bairui Square, ShiXinbei Road, XiaoShan District, HangZhou China.

Baig, H., Keith, C., Heasman, B. and Mallick, T.K. (2012) 'Non-uniform illumination in concentrating solar cells', *Renewable and Sustainable Energy Review*, Vol. 16, No. 8, pp.5890–5909.

Baig, H., Sellami, N. and Mallick, P.K. (2015) 'Performance modeling and testing of a building integrated concentrating photovoltaic (BICPV) system', *Solar Energy Materials and Solar Cells*, Vol. 134, pp.29–44.

Cardona, S.P.P. (2001) '*Coupling of Photocatalytic and Biological Processes as a Contribution to the Detoxification of Water: Catalytic and Technological Aspects*, PhD Thesis, Federal Institute of Technology in Lausanne (EPFL), Switzerland.

Chemisana, D. (2011) 'Building integrated concentrating photovoltaics: a review', *Renewable and Sustainable Energy Reviews*, Vol. 15, No. 1, pp.603–611.

De Boer, B.J., Sinke, W.C., Oldenkamp, H. and De Jong, I. (2003) 'PV-wirefree: bringing PV-systems back to their essentials', A paper presented at the *3rd World Conference on Photovoltaic Energy Conversion*, 11–18 May, Osaka, Japan.

Edenburn, M.W. and Burns, J.R. (1981) 'Shading analysis of a photovoltaic cell string illuminated by a parabolic through concentrator', *Proceedings of the 15th IEEE Photovoltaic Specialists Conference*, 12–15 May, Kissimmee, Florida, USA, pp.63–68.

Gajbert, H., Hall, M. and Karlsson, B. (2007) 'Optimisation of reflector and module geometrics for stationary low-concentrating facade-integrated photovoltaic systems', *Solar Energy Materials and Solar Cells*, Vol. 91, No. 19, pp.1788–1799.

Greenman, P. (1980) 'Reduction of intensity variations on the absorbers of ideal flux concentrators', *Applied Optics*, Vol. 19, No. 16, pp.281–289.

Guiqiang, L., Gang, P., Yuehong, S., Jie, J. and Riffat, S.B. (2013) 'Experiment and simulation study on the flux distribution of lens-walled compound parabolic concentrator compared with mirror compound parabolic concentrator', *Energy*, Vol. 58, pp.398–403.

Gupta, A., Murlidhar, K.S. and Tewery, V.K. (1981) 'Design and testing of a uniformly illumination non-tracking concentrator', *Solar Energy*, Vol. 27, No. 5, pp.387–391.

Hall, M., Roos, A. and Karlsson, B. (2005) 'Reflector materials for two-dimensional low-concentrating photovoltaic systems: the effect of specular versus diffuse reflectance on the module efficiency', *Progress in Photovoltaics: Research and Applications*, Vol. 13, No. 3, pp.217–233.

Hatwaambo, S., Hakansson, H., Nilsson, J. and Karlsson, B. (2008) 'Angular characterisation of low concentrating PV-CPC using low-cost reflectors', *Solar Energy Materials and Solar Cells*, Vol. 92, No. 11, pp.1347–1351.

Jorgensen, G. and Wendelin, T. (1992) *Uniform Flux Dish Concentrators for PV Application*, National Renewable Energy Laboratory, NREL/TP-441-4800, U.S Department of Energy, Colorado, USA.

Kurzweg, U.H. (1980) 'Class of axisymmetric mirrors with uniform flux concentration properties along their axes', *Journal of Optical Society of America*, Vol. 70, No. 6, pp.750–752.

Liu, J., Yao, Y., Xiao, S. and Gu, X. (2018) 'Review of status developments of high-efficiency crystalline silicon solar cells', *Journal of Physics D: Applied Physics*, Vol.51, No. 12, Article ID: 123001.

Luque, A., Sala, G. and Luque-Heredia, I. (2006) 'Photovoltaic concentration at the onset of its commercial deployment', *Progress in Photovoltaics: Research and Applications*, Vol. 14, No. 5, pp.413–428.

Maiti, S., Sarmah, N., Bapat, P. and Mallick, T.K. (2012) 'Optical analysis of a photovoltaic V-trough system installed in western India', *Applied Optics*, Vol. 51, No. 36, pp.8606–8614.

Mallick, T.K. and Eames, P.C. (2007) 'Design and fabrication of low concentrating second generation PRIDE concentrator', *Solar Energy Materials and Solar Cells*, Vol. 91, No. 7, pp.597–608.

Mallick, T.K., Eames, P.C. and B. Norton, B. (2006) 'Non-concentrating and asymmetric compound parabolic concentrating building façade integrated photovoltaics: an experimental comparison', *Solar Energy*, Vol. 80, No. 7, pp.834–849.

Mallick, T.K., Eames, P.C., Hyde, T.J. and Norton, B. (2004) 'The design and experimental characterisation of an asymmetric compound parabolic photovoltaic concentrator for building façade integration in the UK', *Solar Energy*, Vol. 77, No. 3, pp.319–327.

Mallick, T.K., Eames, P.C., Hyde, T.J. and Norton, B. (2007) 'Power losses in an asymmetric compound parabolic photovoltaic concentrator', *Solar Energy Materials and Solar Cells*, Vol. 91, No. 12, pp.1137–1146.

Mammo, E.D., Sellami, N. and Mallick, T.K. (2012) 'Performance analysis of a reflective 3D crossed compound parabolic concentrating photovoltaic system for building façade integration', *Progress in Photovoltaics: Research and Applications*, Vol. 21, No. 5, pp.1095–1103.

Micheli, L., Sarmah, N., Luo, X., Reddy, K.S. and Mallick, T.K. (2013) 'Opportunities and challenges in micro- and nano-technologies for concentrating photovoltaic cooling: a review', *Renewable and Sustainable Energy Reviews*, Vol. 20, pp.595–610.

Muhammad-Sukki, F., Abu-Bakar, S.H., Ramirez-Iniguez, R., McMeekin, S.G., Stewart, B.G., Sarmah, N., Mallick, T.K., Munir, A.B., Mohd-Yasin, S.H. and Abdul, R.R. (2014) 'Mirror symmetrical dielectric totally internally reflecting concentrator for building integrated photovoltaic systems', *Applied Energy*, Vol. 113, pp.32–40.

Nasby, R.D. and Sanderson, R.W. (1982) 'Performance measurement techniques for concentrated photovoltaic cells', *Solar Cells*, Vol. 6, No. 1, pp.39–47.

Nilsson, J., Leutz, R. and Karlsson, B. (2007) 'Micro-structured reflector surfaces for a stationary asymmetric parabolic solar concentrators', *Solar Energy Materials and Solar Cell*, Vol. 16 No. 6, pp.525–533.

Osterwald, C.R., Adelstein, J., Del-Cueto, J.A., Sekulic, W., Trudell, D., McNutt, P., Hansen, R., Rummel, S., Anderberg, A. and Moriarty, T. (2006) 'Resistive loading of photovoltaic modules and arrays for long-term exposure testing', *Progress in Photovoltaics: Research and Applications*, Vol. 14, No. 6, pp.567–575.

Paul, D.I. (2011) *Characterisation of Solar Concentrating Systems for Photovoltaics and their Impact on Performance*, PhD Thesis, University of Ulster, UK.

Paul, D.I., Smyth, M. and Zacharopoulos, A. (2019) 'The effect of non-uniformities in temperature on the performance parameters of an isolated cell photovoltaic module with a compound parabolic concentrator', *International Journal of Renewable Energy Technology*, Vol. 10, Nos. 1/2, pp.3–25.

Paul, D.I., Smyth, M., Zacharopoulos, A. and Mondol, J. (2013) 'The design, fabrication and indoor experimental characterisation of an isolated cell photovoltaic module', *Solar Energy*, Vol. 88, pp.1–12.

Pfeiffer, H. and Bihler, M. (1982) 'The effects of non-uniform illumination of solar cells with concentrated light', *Solar Cells*, Vol. 5, pp.293–299.

Prapas, D.E., Norton, B. and Probert, S.D. (1987) 'Thermal design of compound parabolic concentrating solar energy collectors', *Transactions of the ASME Journal of Solar Energy Engineering*, Vol. 109, pp.161–168.

Rabl, A. (1976) 'Optical and thermal properties of compound parabolic concentrators', *Solar Energy*, Vol. 18, pp.497–511.

Rauschenbach, H.S. (1980) *Solar Cell Array Design Handbook*, *Principles and Technology of Photovoltaic Energy Conversion*, Van Nostrand Reinhold Co., New York, USA.

Reijenga, T. (2000) 'Photovoltaic building integration concepts – what do architects needs?', *Proceedings of the IEA PVPS Task VII Workshop: Featuring a Review on PV Products*, 11–12 February, Lausanne, Switzerland.

Sellami, N. and Mallick, T.K. (2013) 'Optical characterisation and optimisation of a static Window integrated concentrating photovoltaic system', *Solar Energy*, Vol. 91, pp.273–282.

Sellami, N., Mallick, T.K. and McNeil, D.A. (2012) 'Optical characterisation of 3-D static solar concentrator', *Energy Conversion and Management*, Vol. 64, pp.579–586.

Sharma, S., Tahir, A., Reddy, S.K. and Mallick, T.K. (2016) 'Performance enhancement of a building-integrated concentrating photovoltaic system using phase change material', *Solar Energy Materials and Solar Cells*, Vol. 149, pp.29–39.

Singh, P. and Liburdy, J.A. (1993) 'Solar concentrator design for uniform flux on a flat receiver', *Energy Conversion and Management*, Vol. 34, No. 7, pp.533–543.

Suryanto-Hasyim, E., Wenham, S.R. and Green, M.A. (1986) 'Shadow tolerance of modules incorporating integral bypass diode solar cells', *Solar Cells*, Vol. 19, No. 2, pp.109–122.

Swanson, R.M. (2003) 'Photovoltaic concentrators (Chapter 11)', in Luque, A. and Hegedus, S.S. (Eds.): *Handbook of Photovoltaic Science and Engineering*, John Wiley and Sons Ltd., UK.

Tripanagnostopoulos, Y., Georgostathis, P. and Iliopoulou, A. (2009) 'Optical study of new designs for CPVT systems', A paper represented at the *2nd International Workshop on Concentrating Power Plants: Optical Design and Grid Connection*, 9–10 March, Darmstadt, Germany.

Tripanagnostopoulou, M. and Tripanagnostopoulou, Y. (2008) 'Building integrated solar collectors and photovoltaics, an energy solution with aesthetic and environmental benefits, A paper presented at the *Conference for Sustainable Building Event for the Mediterranean Region (SB08MED&EXPO)*, 10–12 January, Athens, Greece.

Whitfield, G.R., Bentley, R.W., Weatherby, C.K., Hunt, A.C., Mohring, H.D., Klotz, F.H., Keuber, P., Minano, J.C. and Alarte-Garvi, E. (1999) 'The development and testing of small concentrating PV systems', *Solar Energy*, Vol. 67, Nos. 1–3, pp.23–34.

Xuan, Q., Li, G., Pei, G., Su, Y. and Ji, J. (2017) 'Design and optical evaluation of a novel asymmetric lens-walled compound parabolic concentrator integration with building south wall', *Journal of Daylighting*, Vol. 4, pp.26–36.

Yamamoto, K., Yoshikawa, K., Uzu, H. and Adachi, D. (2018) 'High-efficiency heterojunction crystalline Si solar cells', *Japanese Journal of Applied Physics*, Vol. 57, pp.08RB20-1–08RB20-8.

Zacharopoulos, A. (2001) *Optical Design Modelling and Experimental Characterisation of Line-Axis Concentrators for Solar Photovoltaic and Thermal Applications*, PhD Thesis, University of Ulster, UK.

Zacharopoulos, A., Eames, P.C., McLarnon, D. and Norton, B. (2000) 'Linear dielectric non-imaging concentrating covers for PV integrated building facades', *Solar Energy*, Vol. 68, pp.439–452.